Chapter 1

Synthesis and Application of Copper Nanowires and Silver Nanosheet-Coated Copper Nanowires as Nanofillers in Several Polymers

Ningning Zeng, Shuguang Fan, Jingyi Ma, Yujuan Zhang, Shengmao Zhang, Pingyu Zhang and Zhijun Zhang

Additional information is available at the end of the chapter

http://dx.doi.org/10.5772/67782

Abstract

A large amount of copper (Cu) nanowires was synthesized through the reduction of $Cu(OH)_2$ by hydrazine in an aqueous solution containing NaOH and ethylenediamine. Besides, Cu nanowires coated by silver nanosheet (denoted as Cu@Ag nanowires) were prepared with a facile transmetalation reaction method. In the meantime, the as-prepared Cu and Cu@Ag nanowires were used as the nanofillers of polyvinyl chloride (PVC), ultra-high molecular weight polyethylene (UHMWPE) and epoxy resin (EP), and their effects on the thermal properties and mechanical properties as well as friction and wear behavior of the polymer-matrix composites nanocomposites were examined. Results indicate that the as-prepared Cu@Ag nanowires consist of Cu nanowires core and Ag nanosheet shell. The Ag nanosheet shell can well inhibit the oxidation of the Cu nanowires core, thereby providing the as-prepared Cu@Ag nanowires with good thermal stability even at an elevated temperature of 230°C. As compared with Cu nanowires, Cu@Ag nanowires could effectively increase the thermal stability of the PVC matrix composites. Moreover, due to the special morphology and microstructure, the as-prepared Cu@Ag nanowires can effectively improve the mechanical properties and wear resistance of PVC, UHMWPE, and EP.

Keywords: Cu nanowires, Cu@Ag nanowires, nanocomposite, mechanical properties, tribological properties

1. Introduction

Copper nanowires could have promising applications in electronics [1–6], optoelectronics [7], solar cells [8–10], photonics, magnetics, genetic engineering, chemical sensors, and lubrication [11, 12], due to their unique characteristics such as high electrical conductivity and thermal conductivity as well as high aspect ratio and tribological properties. Particularly, copper nanowires often can effectively improve the mechanical properties, thermal properties, and wear resistance of polymers such as polystyrene [13, 14] and polyamide 6 [15, 16].

A variety of methods such as solution-phase method and complex-surfactant-assisted hydrothermal reduction approach are currently available for the synthesis of Cu nanowires [17–35]. Here the solution-phase method uses hydrazine (N_2H_4) to reduce Cu^{2+} ions in the highly basic aqueous solution of copper nitrate ($Cu(NO_3)_2$) at 25–100°C in the presence of ethylenediamine (EDA, $C_2H_8N_2$) as the surface-capping agent [32, 33]. The resultant Cu nanowires have a length of >40 μm and a diameter in the range of 60–160 nm, where a high concentration of NaOH (pH = 13–14) is required to prevent copper ions from forming copper hydroxide precipitates. The so-called complex-surfactant-assisted hydrothermal reduction approach can achieve facile synthesis of metal copper nanowires with an average diameter of 85 nm and a length of several tens of micrometers [34], where the copper nanowires are formed through the reduction of CuII−glycerol complex ($Cu(C_3H_6O_3)$) by phosphite (HPO_3^{2-}) at 120°C in the presence of surfactant sodium dodecyl benzenesulfonate (SDBS).

The synthesis and application of Cu nanowires, however, are still challenging because Cu nanowires are liable to spontaneous oxidation in air. Therefore, it is imperative to adopt carbon materials [36–39], polymers [40], and metals [10, 41–45] as the sources to introduce nonoxidizable shells on the surface of Cu nanowires, thereby preventing them from oxidation.

Among various surface-capped Cu nanowires, the metal-capped ones are of special interest, because they can be well prevented from oxidation while basic characteristics of metals are retained. We are particularly interested in Ag as a potential surface-capping shell of Cu nanowires. This is because, with thermal conductivity and electrical conductivity similar to that of Cu, Ag exhibits excellent oxidation resistance [46–51]. A couple of Ag-capped Cu nanowires have been reported elsewhere, mainly involving Cu nanowires-Ag nanowires synthesized in solution phase by the heterogeneous nucleation and growth of Ag nanocrystals on presynthesized Cu nanowires [50] and Cu@Ag nanowires with rough surface obtained by the transmetalation reaction at the room temperature [51]. The Cu nanowire cores of these Ag-capped Cu nanowires indeed can be well prevented from oxidation. However, the Ag shell of Cu@Ag nanowires consists of Ag nanoparticles, which is unfavorable for achieving full contact between the nanofillers and polymer matrix.

http://dx.doi.org/10.5772/67782

Therefore, in the present research, we prepare Ag nanosheets on Cu nanowires, hoping to achieve a large contact area between the nanofillers and polymer matrix, thereby acquiring improved mechanical properties and wear resistance. This article reports the preparation of Cu@Ag nanowires as well as the evaluation of their oxidation resistance. Besides, it also deals with the effect of Cu@Ag nanowires on the mechanical properties, thermal properties, and wear resistance of polyvinyl chloride (PVC), ultrahigh molecular weight polyethylene (UHMWPE), and epoxy resin (EP).

2. Preparation and characterization of Cu nanowires

Cu nanowires were prepared through the reduction of $Cu(OH)_2$ by hydrazine in an aqueous solution containing NaOH and ethylenediamine (EDA), with which the approach developed by Zeng et al. was modified to scale up the reaction by 3900 times (yield of Cu nanowires from 0.006 g to 23.5 g of) for potential large-scale production [30]. Briefly, NaOH (18 L, 7 M), $Cu(OH)_2$ (0.36 mol), EDA (135 mL), and hydrazine (18 mL, 35 wt.%) were added to a 20 L reactor and heated at 80°C for 30 min to achieve the reduction of Cu^{2+} to metallic copper at a rate of 100% (**Figure 1**). The as-prepared Cu nanowire cake is present on the top of the solution, possibly due to the entrapping of nitrogen bubbles among the nanowires ($2Cu^{2+} + N_2H_4 + 4OH^- \rightarrow 2Cu + N_2 + 4H_2O$). **Figure 1a** shows the scanning electron microscopic (SEM) images of the as-prepared Cu nanowires. They are straight and have a diameter of 150–200 nm and a length of about 10 μm. **Figure 1b** shows the X-ray diffraction (XRD) pattern of the Cu nanowires. The peaks at 2θ = 43.3, 50.4, 74.1, and 89.9° correspond to the (1 1 1), (2 0 0), (2 2 0), and (3 1 1) crystal planes of cubic Cu (PDF No. 89-2838), which indicates that the copper nanowires exhibit face-centered cubic (fcc) structure. No XRD signals of other species are detected, which indicate that the as-prepared Cu nanowires are highly pure. However, when the as-prepared Cu nanowires are placed in air for 24 h, three XRD peaks emerge at 2θ = 36.4, 42.3 and 52.5° (**Figure 1c**), and they correspond to the (1 1 1), (2 0 0), and (2 1 1) crystal planes of Cu_2O (PDF No. 78-2076). This means that the as-prepared Cu nanowires are easily oxidized in air environment.

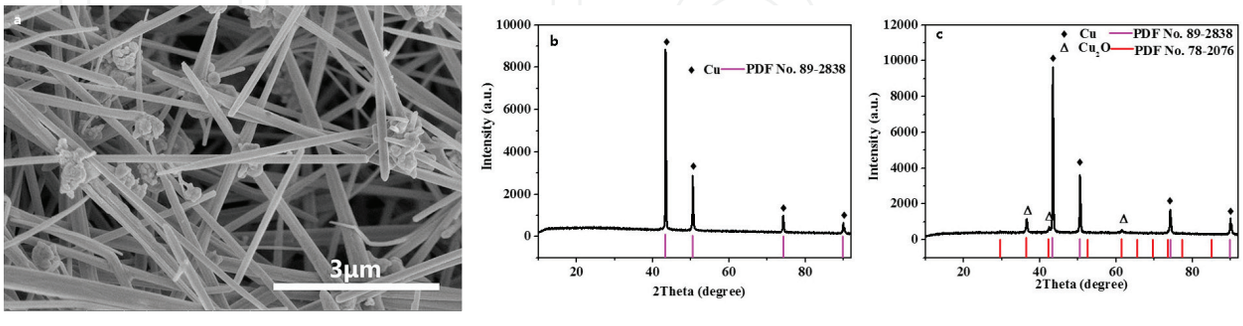

Figure 1. (a) SEM image of as-prepared Cu nanowires in mother liquor and XRD patterns, (b) as-prepared Cu nanowires, and (c) Cu nanowires after being stored in air for 24 h.

3. Preparation and characterization of Cu@Ag nanowires

The formation of Cu@Ag nanowires by the transmetalation reaction should be closely related to the different reduction potentials of Cu and Ag. First, 1.5 mmol $AgNO_3$ was dispersed in distilled water. Into the $AgNO_3$ solution was dropwise added the ammonium hydroxide (NH_4OH, 28–30%, BDH) aqueous solution under vigorous stirring until the yellow precipitate disappeared and the solution became clear. The as-obtained Ag-amine reagent solution was then directly added into 50 mL of Cu nanowires dispersion (with 0.5 g of Cu nanowires) under vigorous magnetic stirring at 40°C. After 2 h of reaction, the as-obtained product was washed with deionized water and collected by centrifugation, followed by redispersion in deionized water. During the synthesis progress, the Cu atoms on the surface of Cu nanowires quickly react with Ag^+ ions to release Cu^{2+}. Simultaneously, Ag^+ ions are reduced into Ag atoms and deposited on the surface of the Cu nanowires, during which the color of Cu nanowires dispersion turns grey along with the appearance of metallic Ag. Therefore, the morphology and microstructure of the as-prepared Cu@Ag nanowires should be highly dependent on the reaction conditions. Through comprehensive analysis, the optimal reaction condition is that temperature is 40°C; Cu/Ag molar ratio is 5:1; Cu dispersion concentration is 1% and silver ammonia reagent dropping speed is poured directly.

Figure 2 shows the SEM and TEM images as well as XRD pattern and EDS line map of the Cu@Ag nanowires prepared under the optimal reaction condition. It can be seen that the as-prepared Cu@Ag nanowires have a diameter of about 250 nm and a length of about 10 μm (**Figure 2a**). Besides, the major XRD peaks of the as-prepared Cu@Ag nanowires can be indexed to metallic Ag (PDF No. 87-0717) and Cu (PDF No. 89-2838) with fcc structure (**Figure 2b**). The

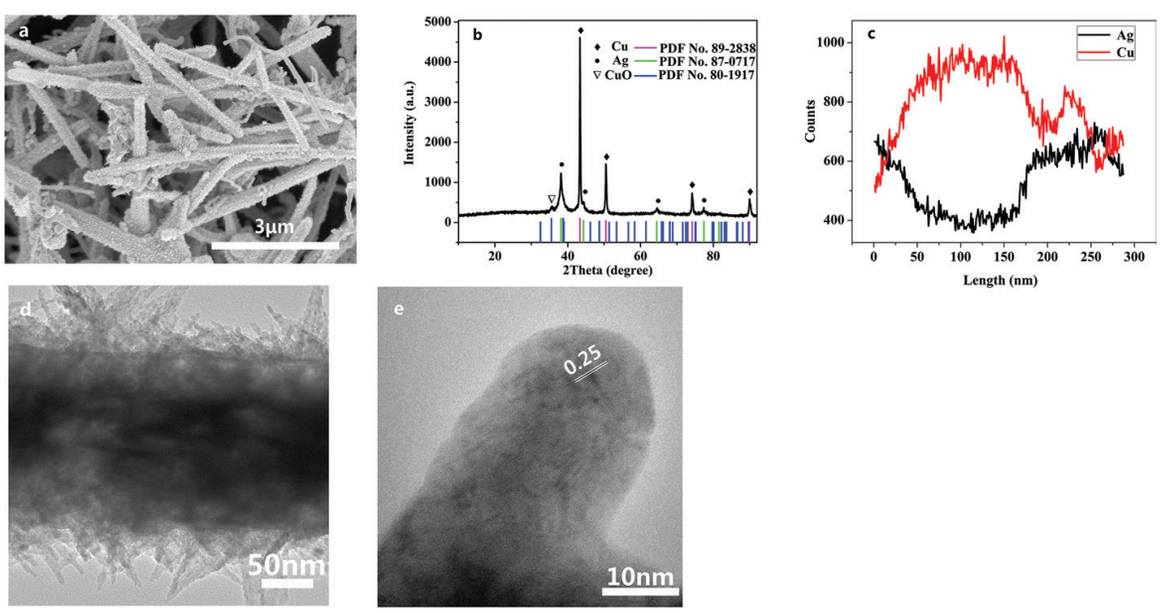

Figure 2. Characterization of Cu@Ag nanowires prepared under the optimal reaction condition: (a) SEM image, (b) XRD pattern, (c) EDS line map, (d) TEM image, and (e) HRTEM image.

small peak at $2\theta = 35.5°$ can be indexed to CuO (PDF No. 80-1917), which is possibly due to the oxidation of original Cu nanowires before coating with Ag nanosheets. In terms of the element line distribution, the copper element has a maximum value at the center part whereas the Ag shows a complementary profile with two maxima on both sides (**Figure 2c**). This indicates that the as-prepared Cu@Ag nanowires have a core-shell structure composed of Cu core and Ag shell. Such a core-shell structure of the as-prepared Cu@Ag nanowires is also supported by corresponding TEM image shown in **Figure 2d**. Namely, there is a layer of Ag nanosheets on Cu nanowires. Moreover, the high-resolution TEM (HRTEM) image of Cu@Ag nanowires indicates that the Ag crystal exhibits a fringe lattice spacing of 0.25 nm (**Figure 2e**), and it corresponds to the (200) plane of the Ag crystal.

The thermal stability of Cu@Ag nanowires with different treatments was measured by XRD. **Figure 3a** shows the XRD pattern of Cu@Ag nanowires prepared under the optimal condition after 2 month of storage in ambient condition. All the characteristic peaks remain unchanged after 2 month of storage in air, which indicates that the Ag shell layer can well inhibit the oxidation of the Cu nanowires core. **Figure 3b** shows the XRD patterns of the same product after being sintered at different temperatures. It can be seen that the XRD patterns have no change before 200°C contrasted with the XRD of as-prepared samples, while after being sintered at 300°C, a distinct peak of Cu_2O emerges and the major peaks of metallic Cu and Ag still remain, which indicates the Ag coating can protect Cu nanowires core from oxidation at high temperature. This means that the Cu@Ag nanowires show better thermal stability than Cu nanowires.

In order to further determine oxidation resistance of Cu@Ag nanowires, TG analysis was conducted in air flow. **Figure 4** shows the TG curves of the as-prepared Cu nanowires and Cu@Ag nanowires in air. The TG curves show Cu nanowires undergo a weight-gain around 100°C attributed to the oxidation thereat, while the Cu@Ag nanowires began to add the weight at around 230°C indicating that Cu@Ag nanowires have the higher oxidation resistance temperature, which also demonstrates that Cu@Ag nanowires exhibit much better thermal stability than Cu nanowires.

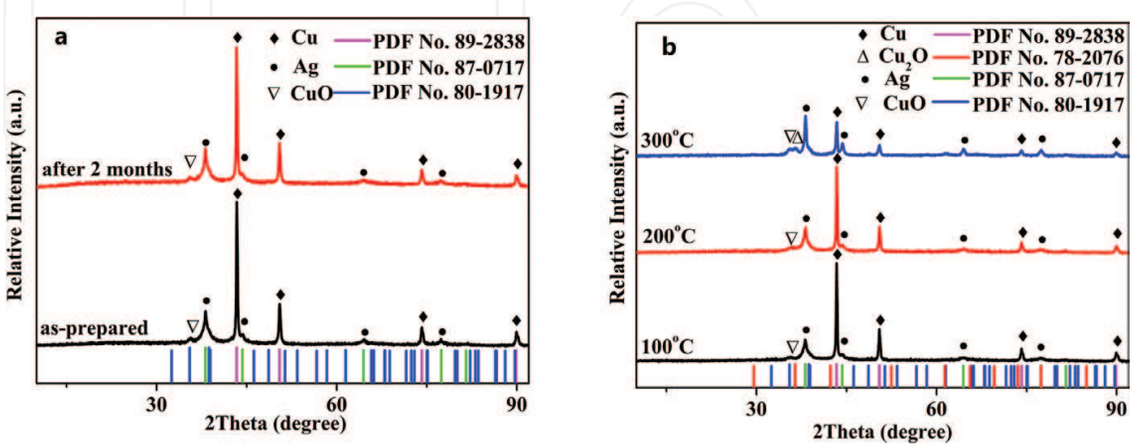

Figure 3. XRD paterns of Cu@Ag nanowires prepared under the optimal reaction condition: (a)after storage for different times in air, (b) after being sintered at different temperatures.

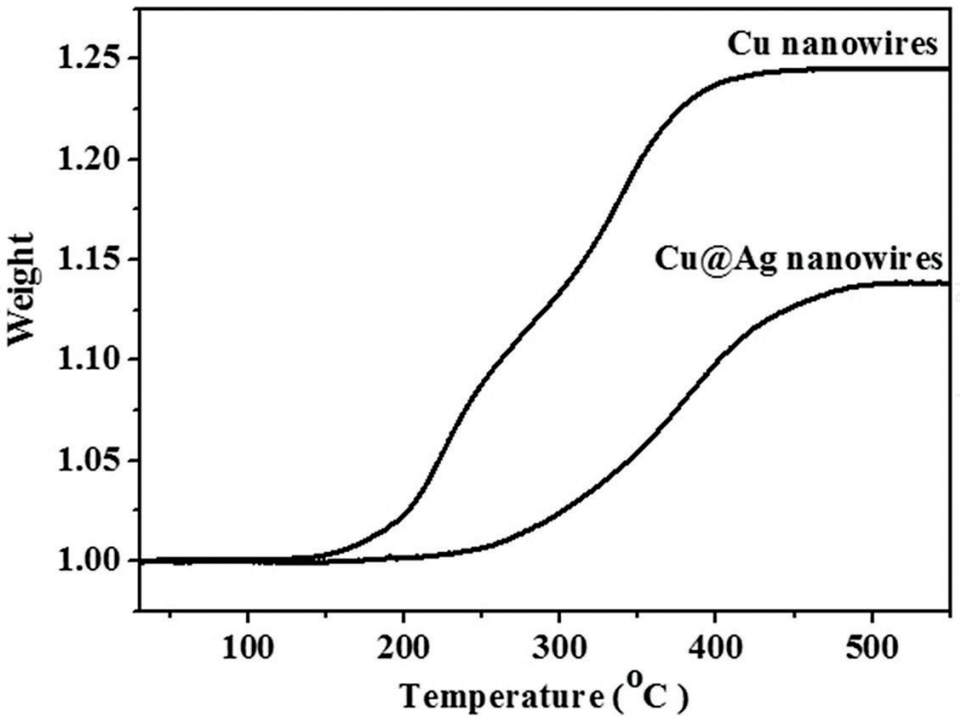

Figure 4. TG curves of Cu nanowires and Cu@Ag nanowires in air at a heating rate of 10°C/min.

4. Cu/Cu@Ag nanowires-PVC nanocomposites

The component and dosage for the preparation of Cu/Cu@Ag nanowires-PVC composites materials are listed in **Table 1**. The raw materials were mixed with mechanical stirring for 20 min, then melt blended by a laboratory two roll mill with a rotate speed of 50 rpm under 100°C for 10 min. The milled sheets were compressed by a press machine at 175°C and 20 MPa for 5 min. The samples for performance test were cut from the final sheets.

Nano-filler mass fraction (%)	Component (g)					
	PVC	Octadecanoic acid	Lead stearate	Calcium stearate	Dioctyl phthalate	Cu/Cu@Ag nanowires
0	160	1.28	0.64	0.64	32	0
0.1	160	1.28	0.64	0.64	32	0.195
0.5	160	1.28	0.64	0.64	32	0.978
1.0	160	1.28	0.64	0.64	32	1.97
3.0	160	1.28	0.64	0.64	32	6.02

Table 1. The component and dosage for the preparation of Cu nanowires- and Cu@Ag nanowires-PVC composites.

4.1. Thermal properties of Cu/Cu@Ag nanowires-PVC nanocomposites

Thermal properties of the composites were studied by differential scanning calorimetry (DSC). DSC curves were obtained by heating at 10°C/min rate under N_2 at a flow rate of 100 mL/min in the range of 20–120°C by using NETZSCH DSC 204HP instrument (Bavarian, Germany). The heated sample was cooled to 20°C and reheated for the second time using the same heating program.

An exemplary DSC heating curve for Cu nanowires-PVC nanocomposites is presented in **Figure 5**, with the indication of the procedure of glass transitions temperatures (Tg) determination as a central point value of the tangent line to the DSC curve, at the inflection point where the characteristic augment of the base line, related to the increase of the specific heat, was used for the determination of the glass transition. For all samples, the run of the DSC curve at the domain of the glass transition was similar.

The Tg of the Cu@Ag nanowires-PVC nanocomposites is presented in **Figure 6**. It can be seen that, as compared with Cu nanowires, the introduction of Cu@Ag nanowires results in a larger increase in the Tg value. Besides, the Tg of the Cu@Ag nanowires-PVC nanocomposites tends to rise with the increase of Cu@Ag nanowire content. This is because, with the increase of the Cu@Ag nanowire content, more Cu@Ag nanowires act as physical cross-linkers to be intertwined with macromolecular chains, thereby reducing the chain segmental mobility of PVC and increasing the Tg. However, when the content of Cu@Ag nanowires

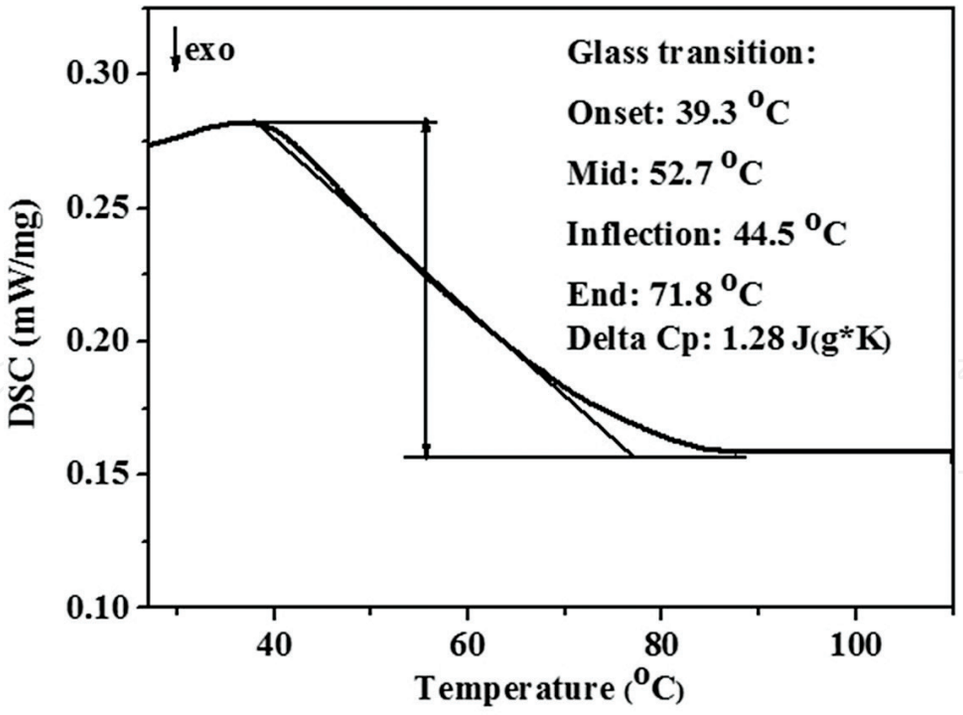

Figure 5. An exemplary DSC trace for Cu nanowires-PVC composite (Cu nanowires contain: 1 wt.%) at the domain of the glass transition.

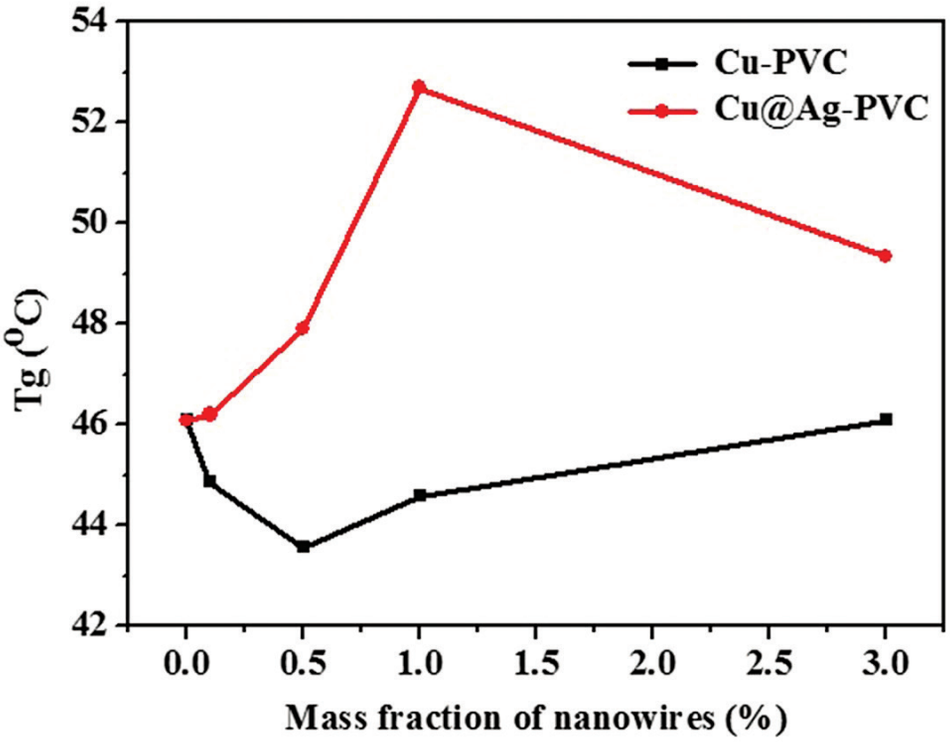

Figure 6. The glass transition temperature (Tg) of Cu/Cu@Ag nanowires-PVC nanocomposites with various mass fractions of the nanofillers.

is too high, the Tg values of the PVC-matrix nanocomposites declines to some extent. The reason lies in that a too high content of Cu@Ag nanowires would tend to agglomerate in the polymer matrix and weaken the interaction with the macromolecular chains, thereby limiting the movements of the macromolecular chains and reducing the Tg value of the PVC-matrix nanocomposites. Moreover, the presence of Cu@Ag nanowires in PVC matrix contributes to increasing the elasticity especially in the glass transition region, which corresponds to enhanced thermal stability of the PVC-matrix nanocomposites.

4.2. Mechanical properties of Cu/Cu@Ag nanowires-PVC nanocomposites

Mean values of five factors on mechanical properties were analyzed in this work. The tensile strength and elongation at break of these samples are shown in **Figure 7**. From **Figure 7**, it can be seen that the elongation at break of composite materials all increase to varying degrees by addition of the nanowires. And the effect of Cu@Ag nanowires is much larger than the Cu nanowires. Meanwhile, the tensile strength keeps no change on the whole.

4.3. Tribology properties of Cu/Cu@Ag nanowires-PVC nanocomposites

Figure 8 shows the friction coefficient and wear rate of Cu/Cu@Ag nanowires-PVC nanocomposites (load: 20 N; route: 5 mm; frequency: 2 Hz; time: 5 min; room temperature). The friction coefficient of Cu/Cu@Ag nanowires PVC nanocomposites has little change with

http://dx.doi.org/10.5772/67782

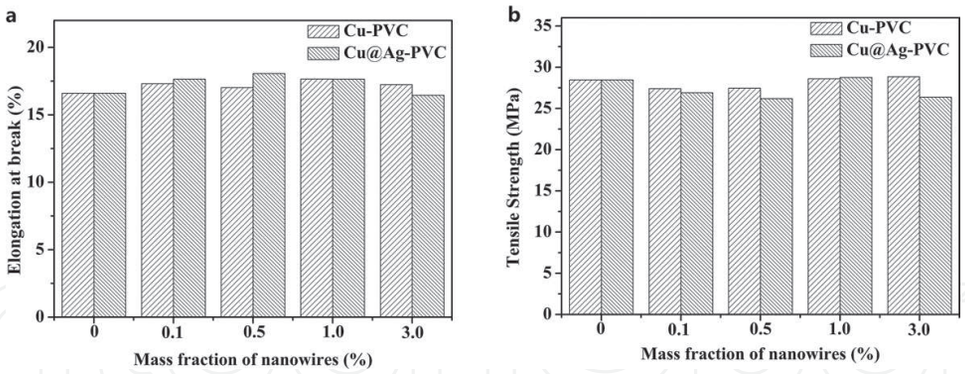

Figure 7. The elongation at break (a) and tensile strength and (b) Cu/Cu@Ag nanowires-PVC nanocomposites with different nanowires contents.

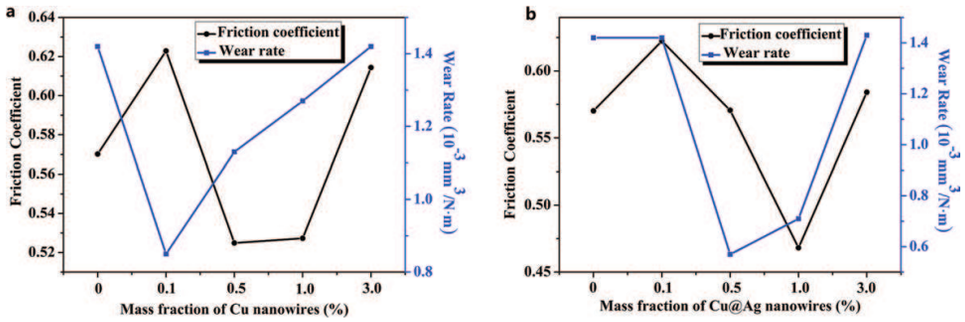

Figure 8. The friction and wear behavior (friction coefficient and wear rate) of PVC nanocomposites with different contents of (a) Cu nanowires and (b) Cu@Ag nanowires.

increasing amount of copper nanowire, while the wear rate changes greatly therewith. Namely, pure PVC (without Cu nanowires) has a larger wear rate as much as 1.42×10^{-3} mm^3/N m, while PVC composite containing 0.5 wt.% Cu@Ag nanowires has an obviously reduced wear rate of 0.57×10^{-3} mm^3/N m (reduced by nearly 60%). It can be clearly seen that lower or higher concentrations of fillers in the matrix are less effective in reducing the friction coefficient and wear rate. It can be inferred that, at a too low concentration, the nanofillers can hardly play its role on the friction-reducing and wear resistance in the friction process, thereby leading to relatively not very good friction property. When the additive concentration is too high, the nanofiller would tend to agglomerate and form a large number of weak interfaces in the matrix, which makes the nanofillers easily fall off from the matrix in the friction process causing a higher abrasive wear [52], thus resulting in relatively poor friction property. Therefore, it is suggested to keep the concentration of the nanofillers in polymer matrix as 0.5 wt.% Cu@Ag nanowires in order to effectively reduce the friction coefficient and wear rate. Moreover, the wear rate of Cu nanowires-PVC nanocomposites tends to decline with the increasing content of the Cu nanowires, and the minimum wear rate (0.85×10^{-3} mm^3/N m) is obtained at a Cu nanowires content of 0.1 wt.%.

5. Cu/Cu@Ag nanowires-UHMWPE nanocomposites

The component and dosage for the preparation of Cu@Ag nanowires-UHMWPE composites are listed in **Table 2**. The nanowires and UHMWPE raw material were mixed with ball milling for 1 h. The mixture was heated to 200°C and pressed under 20 MPa for 10–20 min, followed by cooling to room temperature in the mold to afford the Cu@Ag nanowires-UHMWPE nanocomposites. All the samples for performance test were cut from the final sheets.

5.1. Crystallization and melting behavior of Cu/Cu@Ag nanowires-UHMWPE nanocomposites

The crystallization and melting behavior of Cu/Cu@Ag nanowires-UHMWPE nanocomposites were studied by differential scanning calorimetry (DSC). DSC curves in the range of 20–200°C were measured with a NETZSCH DSC 204HP instrument (Bavarian, Germany) at a heating rate of 10°C/min under N_2 atmosphere (flow rate: 100 mL/min). **Figure 9** shows the crystallization and melting temperature of Cu/Cu@Ag nanowires-UHMWPE nanocomposites. It is seen from **Figure 9a** that Cu nanowires have a strong influence on the crystallization and melting temperature of UHMWPE matrix. When the content of Cu nanowires is 0.1 wt.%, the crystallization temperature of nanocomposite rises from 118.10 to 118.32°C, which could be because that the heterogeneous nucleation in the presence of copper nanowire served as nucleating agent contributes to improving the crystallinity of UHMWPE matrix. With the increasing of nanowires content, the crystallization temperature significantly decreases, which indicates that Cu nanowires hinder the orientation of PA6 crystals and restrict the movement of the molecular chains of UHMWPE. When the nanowires content is further increased, the effect of Cu nanowires on the crystallization and melting behaviors tends to decline, possibly due to the aggregation of the nanofillers in the polymer matrix. When the Cu nanowires content reaches 3 wt.%, however, the crystallization temperature decreases again, probably because that the interaction between excess nanowires and molecular chains of UHMWPE is enhanced to restrict the movement of the molecular chains. Correspondingly, a change in melting temperature occurs with the increasing of nanowires content.

Interestingly, the Cu@Ag nanowires have opposite effects on the crystallization and the melting temperature as compared with Cu nanowires, which could be because the Cu@Ag nanowires

Component	Mass fraction (%)						
	0	**0.1**	**0.3**	**0.5**	**0.8**	**1.0**	**3.0**
UHMWPE (g)	120	120	120	120	120	120	120
Cu/Cu@Ag nanowires (g)	0	0.120	0.361	0.603	0.968	1.21	3.71

Table 2. The component and dosage for the preparation of Cu/Cu@Ag nanowires-UHMWPE composites.

http://dx.doi.org/10.5772/67782

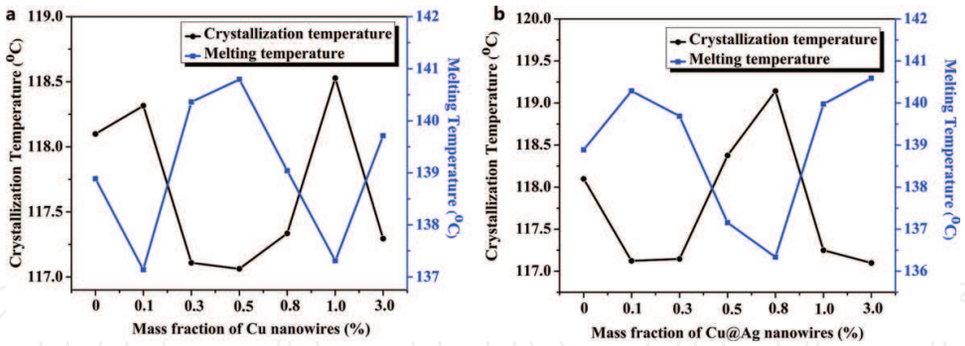

Figure 9. The crystallization and melting temperature of Cu/Cu@Ag nanowires-UHMWPE nanocomposites with different nanowires contents.

with unique morphology and microstructure exhibit significantly increased contact area with the UHMWPE matrix.

5.2. Mechanical properties of Cu/Cu@Ag nanowires-UHMWPE nanocomposites

The effect of Cu/Cu@Ag nanowires on the mechanical properties of UHMWPE is shown in **Figure 10**. We find that the elongation at break of composite materials gradually increases with increasing dosage of Cu/Cu@Ag nanowires; and in particular, the UHMWPE-based nanocomposites with 0.8 wt.% of Cu nanowires or with 0.3 wt.% of Cu@Ag nanowires possesses the maximum values of elongation at break (168 and 190%, respectively), larger than that of unfilled UHMWPE by 78.5 and 101.9% (**Figure 10a**). Besides, the elongation rate at break of the UHMWPE-based nanocomposites tends to decline with further increase of nanowires content, possibly due to the aggregation of the nanowires thereat. Moreover, the elongation rate at break of Cu@Ag nanowires-UHMWPE is higher than that of Cu nanowires-UHMWPE, which could be closely related to the special morphology and microstructure of the Cu@Ag nanowires. Furthermore, the UHMWPE-based nanocomposites change slightly with increasing dosage of Cu/Cu@Ag nanowires. The UHMWPE-based nanocomposites with 0.3 wt.% of Cu nanowires or with 0.5 wt.% of Cu@Ag nanowires possess the maximum values of tensile

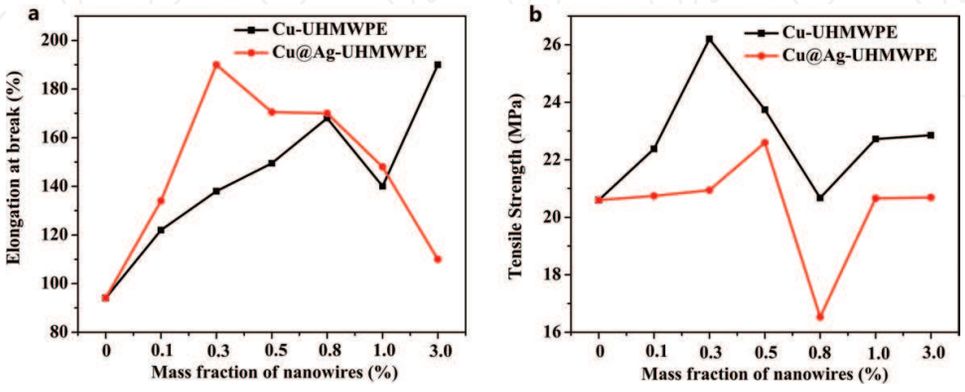

Figure 10. The mechanical properties of Cu/Cu@Ag nanowires-UHMWPE nanocomposites with different nanowires contents.

strength of 26.2 and 22.6 MPa, respectively, showing an increase by 27.1 and 9.7% in comparison with pure UHMWPE (20.6 MPa; **Figure 10b**).

5.3. Tribology properties of Cu/Cu@Ag nanowires-UHMWPE nanocomposites

Figure 11 shows the friction coefficient and wear rate of Cu/Cu@Ag nanowires-UHMWPE nanocomposites (load: 250 N; route: 5 mm; frequency: 2Hz; time: 5 min; room temperature). For Cu nanowires-UHMWPE nanocomposites (**Figure 11a**), the friction coefficient and wear rate of Cu nanowires-UHMWPE nanocomposites gradually decrease with increasing dosage of Cu nanowires; and the friction coefficient is rather large when the Cu nanowires content is below 0.3 wt.%. This may be because that when the content of Cu nanowires is too low to play its role on the friction-reducing and wear resistance in the friction process, thereby leading to relatively not very good friction property. Cu@Ag nanowires-UHMWPE nanocomposites show similar variation tendency as Cu nanowires-UHMWPE nanocomposites (**Figure 11b**) except the one with 3 wt.% of Cu@Ag nanowires is somewhat different.

6. Cu/Cu@Ag nanowires-EP nanocomposites

The Cu/Cu@Ag nanowires-EP (epoxy resin) nanocomposites were prepared by mixing the raw materials with high-speed mixers (1500 rpm, 3 min) in association with curing in the mold under ambient conditions. The content of each component is shown in **Table 3**.

6.1. The electrical conductivity Cu/Cu@Ag nanowires-EP nanocomposites

In general, the electrical conductivity of silver and copper is similar. The special structure of Cu@Ag nanowires makes it feasible to significantly improve the electrical conductivity of Cu nanowires by incorporating Ag shell because of their better oxidation resistance and more conductive network in the polymer matrix nanocomposites. We measured the electrical resistivity of EP-matrix composites filled with Cu and Cu@Ag nanowires using a Hall effect

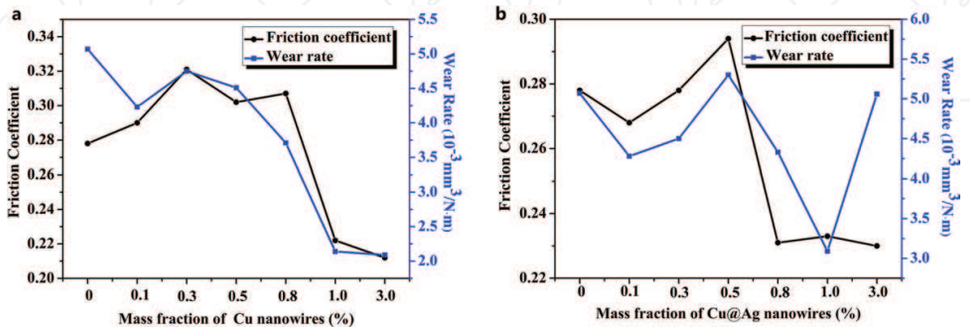

Figure 11. The friction and wear behavior (friction coefficient and wear rate) of UHMWPE nanocomposites with different contents of (a) Cu nanowires and (b) Cu@Ag nanowires.

Component	Mass fraction (%)						
	0	**0.1**	**0.3**	**0.5**	**0.8**	**1.0**	**3.0**
EP (g)	60	60	60	60	60	60	60
Curing agent (g)	15	15	15	15	15	15	15
Cu/Cu@Ag nanowires (g)	0	0.075	0.226	0.377	0.606	0.758	2.320

Table 3. The component and dosage for the preparation of Cu nanowires- and Cu@Ag nanowires-EP composites.

measurement system. The electrical resistivity of pure EP is about 10^{14} Ω cm, while the introduction of Cu/Cu@Ag nanowires results in greatly reduced electrical resistivity (**Figure 12**). Namely, the electrical resistivity decreases obviously with increasing content of Cu or Cu@Ag nanowires, and the EP-matrix nanocomposites filled with Cu@Ag nanowires exhibit lower electrical resistivity than the counterparts filled with Cu nanowires. For example, the resistivity of the EP composite containing 3 wt.% Cu nanowires is about 1.49×10^5 Ω cm, and it does not satisfy the conductive requirement for electrostatic conductive materials (10^4 Ω cm). The resistivity of Cu@Ag nanowires-EP composite (filler mass fraction: 3 wt.%) is reduced to 2.11×10^4 Ω cm, and it satisfies the conductive requirement for electrostatic conductive materials.

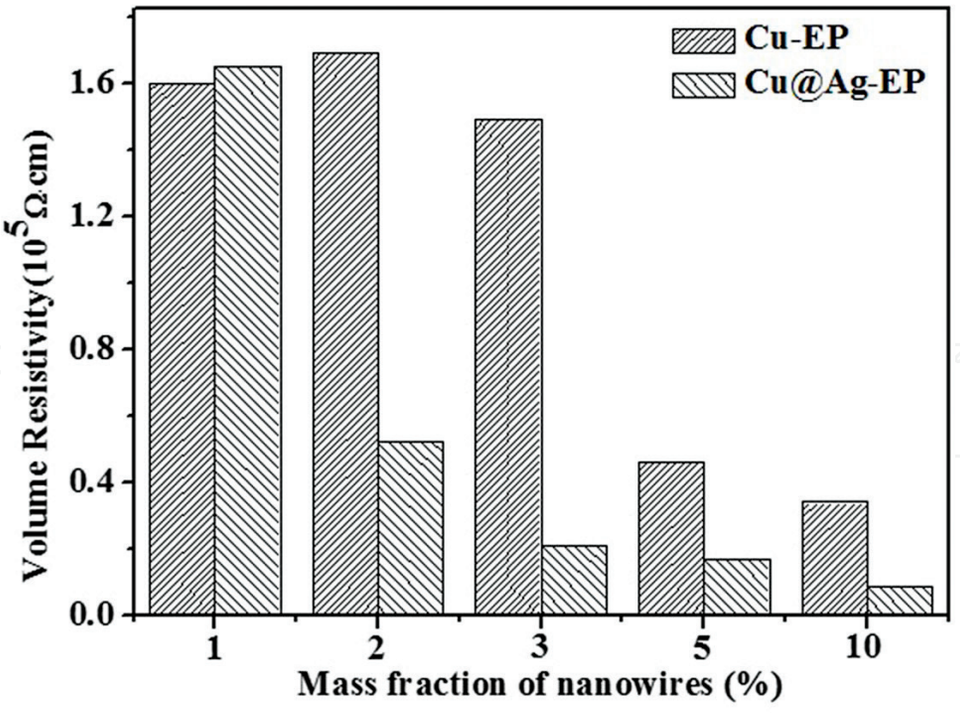

Figure 12. The electrical resistivity of Cu/Cu@Ag nanowires-EP nanocomposites with different nanowires contents.

In other words, encapsulating Cu nanowires with Ag nanosheets makes it feasible for the copper nanowires to be applied as potential electrostatic conductive filler, thereby broadening their application scope.

6.2. Mechanical properties of Cu/Cu@Ag nanowires-EP nanocomposites

The tensile strength and the elongation at break of pure EP and its nanocomposites filled with Cu nanowires or Cu@Ag nanowires are shown in **Figure 13**. Both the tensile strength and elongation at break increase after the introduction of Cu nanowires and Cu@Ag nanowires. Particularly, the EP-matrix nanocomposite with 0.8 wt.% of Cu nanowires exhibits the maximum tensile strength of 74.2 MPa, while the one with 1 wt.% of Cu@Ag nanowires exhibits the maximum tensile strength of 67.5 MPa. In addition, compared with the change of the elongation at break values, the tensile strength has little change with the increase of nanowires content. When the content of the nanowires is too high, the tensile strength and elongation at break are relatively low, which could be due to the aggregation of the nanowires in EP matrix at a high content.

6.3. Tribology properties of Cu/Cu@Ag nanowires-EP nanocomposites

Figure 14 shows the variation in the friction coefficient and wear rate of Cu/Cu@Ag nanowires-EP composites with the content of the nanofillers (load: 20 N; amplitude: 5 mm; frequency: 2Hz; time: 30 min; room temperature). Unfilled EP has a friction coefficient and wear rate of 0.646 and 4.82 × 10^{-3} mm^3/N m. Namely, the EP-matrix nanocomposites with less than 0.5 wt.% of Cu nanowires have reduced friction coefficient and wear rate than neat EP; and in particular, the EP-matrix composite with 0.1% of Cu nanowires exhibits the best friction coefficient and wear rate (0.555, 1.42 × 10^{-3} mm^3/N m; a reduction by 14.1 and 70.5% as compared with that of neat EP). However, the increase in the content of the Cu nanowires above 0.5 wt.% results in increased friction coefficient and wear rate, due to aggregation of the nanofillers thereat. Similar variation tendency is also observed for Cu@Ag nanowires-EP nanocomposites.

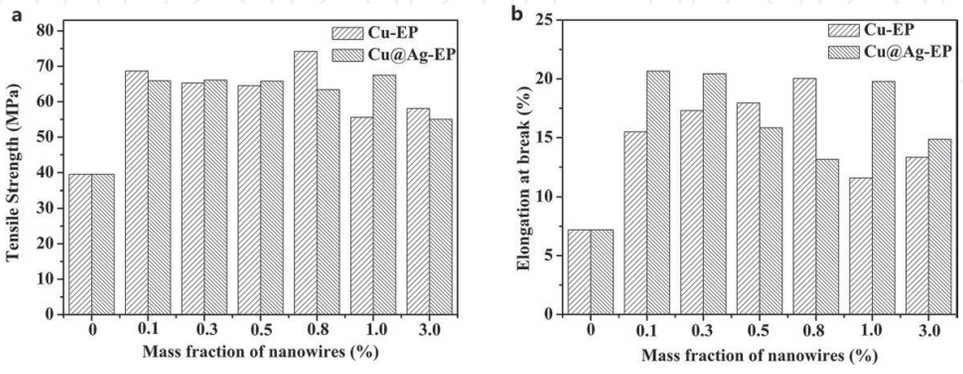

Figure 13. The mechanical properties of Cu/Cu@Ag nanowires-EP nanocomposites with different nanowires content.

http://dx.doi.org/10.5772/67782

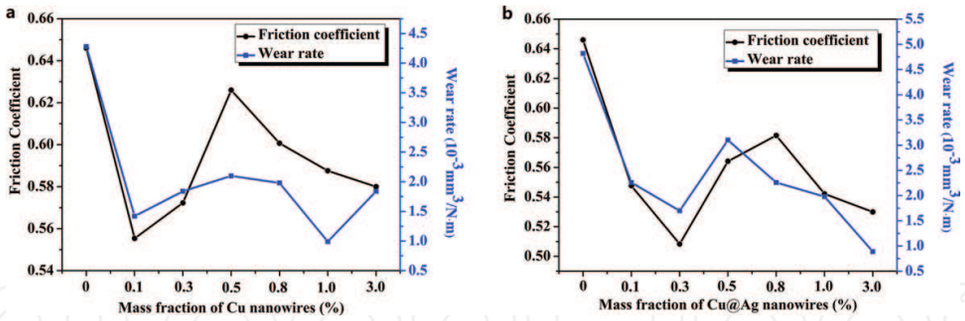

Figure 14. The friction and wear behavior (friction coefficient and wear rate) of EP-matrix nanocomposites with different contents of (a) Cu nanowires and (b) Cu@Ag nanowires.

7. Conclusion

A large amount of Cu nanowires is prepared by a solution-reduction approach, while Cu@Ag nanowires are prepared by a simple and efficient transmetalation reaction method. The morphology and microstructure of the as-prepared Cu@Ag nanowires can be well manipulated by properly adjusting the reaction condition. Resultant Cu@Ag nanowires consist of Cu nanocores and uniformly distributed Ag nanosheet shell, and they exhibit improved thermal stability and electrical conductivity as compared with Cu nanowires, due to the incorporation of the Ag shell. Besides, the as-prepared Cu@Ag nanowires can better improve the mechanical properties and wear resistance than the Cu nanowires.

Acknowledgements

We acknowledge the financial support provided by National Natural Science Foundation of China (Grant no. 51275154, 51405132, 21671053), the Plan for Young Scientific Innovation Talent of Henan Province (Grant no. 154100510018) and Natural Science Foundation of Henan Province (14A150006).

Author details

Ningning Zeng[1], Shuguang Fan[1], Jingyi Ma[1], Yujuan Zhang[1], Shengmao Zhang[1,2]*, Pingyu Zhang[1] and Zhijun Zhang[1]

*Address all correspondence to: zsm@henu.edu.cn

1 Engineering Research Center for Nanomaterials, Henan University, Kaifeng, P. R. China

2 Collaborative Innovation Center of Nano Functional Materials and Applications of Henan Province, Henan University, Kaifeng, P. R. China

References

[1] Hsu P, Wu H, Carney T J. Passivation coating on electrospun copper nanofibers for stable transparent electrodes. ACS Nano. 2012;**6**(6):5150-5156. DOI: 10.1021/nn300844g

[2] Kumar Ravi D V, Woo K, Moon J. Promising wet chemical strategies to synthesize Cu nanowires for emerging electronic applications. Nanoscale. 2015;**7**(41):17195-17210. DOI: 10.1039/c5nr05138j

[3] Yin Z, Lee C, Cho S. Facile synthesis of oxidation-resistant copper nanowires toward solution-processable, flexible, foldable, and free-standing electrodes. Small. 2014;**10**(24):5047-5052. DOI: 10.1002/smll.201401276

[4] He C, Liu G, Zhang W X. Tuning the structures and electron transport properties of ultrathin Cu nanowires by size and bending stress using DFT and DFTB methods. RSC Advances. 2015;**29**(5):22463-22470. DOI: 10.1039/C4RA15051A

[5] Nam V, Lee D. Copper nanowires and their applications for flexible, transparent conducting films: a review. Nanomaterials. 2016;**6**(3):47. DOI:10.3390/nano6030047

[6] Jung S M, Preston D J, Jung H Y. Porous Cu nanowire aerosponges from one-step assembly and their applications in heat dissipation. Advanced Materials. 2016;**28**(7):1413-1419. DOI: 10.1002/adma.201504774

[7] Im H G, Jung S H, Jin J. Flexible transparent conducting hybrid film using a surface-embedded copper nanowire network: a highly oxidation-resistant copper nanowire electrode for flexible optoelectronics. ACS Nano. 2014;**8**(10):10973-10979. DOI: 10.1021/nn504883m

[8] Zhao Y, Zhang Y, Li Y. Rapid and large-scale synthesis of Cu nanowires via a continuous flow solvothermal process and its application in dye-sensitized solar cells (DSSCs). RSC Advances. 2012;**2**(30):11544-11551. DOI: 10.1039/c2ra21224b

[9] Liang J, Bi H, Wan D. Novel Cu nanowires/graphene as the back contact for CdTe solar cells. Advanced Functional Materials. 2012;**22**(6):1267-1271. DOI: 10.1002/adfm.201102809

[10] Stewart I E, Rathmell A R, Yan L. Solution-processed copper–nickel nanowire anodes for organic solar cells. Nanoscale. 2014; **6**(11):5980-5988. DOI: 10.1039/c4nr01024h

[11] Stortini A M, Moretto L M, Mardegan A. Arrays of copper nanowire electrodes: preparation, characterization and application as nitrate sensor. Sensors and Actuators B: Chemical. 2015;**207, Part A**:186-192. DOI: 10.1016/j.snb.2014.09.109

[12] Huang J, Dong Z, Li Y. High performance non-enzymatic glucose biosensor based on copper nanowires–carbon nanotubes hybrid for intracellular glucose study. Sensors and Actuators B: Chemical. 2013;**182**:618-624. DOI: 10.1016/j.snb.2013.03.065

[13] Lin B, Gelves G A, Haber J A. Electrical, morphological and rheological study of melt-mixed polystyrene/copper nanowire nanocomposites. Macromolecular Materials and Engineering. 2008; **293**(7):631-640. DOI: 10.1002/mame.200800045

[14] Gelves G A, Sundararaj U, Haber J A. Electrostatically dissipative polystyrene nanocomposites containing copper nanowires. Macromolecular Rapid Communications. 2005;**26**(25): 1677-1681. DOI: 10.1002/marc.200500490

[15] Xu Q, Li X, Zhang S. Preparation and characterization of copper nanowire/polyamide 6 nanocomposites and its properties. Journal of Macromolecular Science, Part A. 2014;**51**(7):598-603. DOI: 10.1 080/10601325. 2014.916182

[16] Xu Q, Li X, Zhang S. Copper nanowire/PA6 composites prepared by in situ polymerization and its properties. Journal of Polymer Research. 2013;**20**(10):1-6. DOI: 10.1007/s10965-013-0257-7

[17] Cui F, Yu Y, Dou L. Synthesis of ultrathin copper nanowires using tris(trimethylsilyl) silane for high-performance and low-haze transparent conductors. Nano Letters. 2015;**15**(11): 7610-7615. DOI: 10.1021/acs.nanolett.5b03422

[18] Gelves G A, Murakami Z T M, Krantz M J. Multigram synthesis of copper nanowires using ac electrodeposition into porous aluminium oxide templates. Journal of Materials Chemistry. 2006;**16**(30):3075-3083. DOI: 10.1039/b603442j

[19] Inguanta R, Piazza S, Sunseri C. Influence of the electrical parameters on the fabrication of copper nanowires into anodic alumina templates. Applied Surface Science. 2009;**255**(21):8816-8823. DOI: 10.1016/j.apsusc.2009.06.062

[20] Gerein N J, Haber J A. Effect of ac electrodeposition conditions on the growth of high aspect ratio copper nanowires in porous aluminum oxide templates. The Journal of Physical Chemistry B. 2005;**109**(37):17372-17385. DOI: 10.1021/jp051320d

[21] Pate J, Zamora F, Watson S M D. Solution-based DNA-templating of sub-10 nm conductive copper nanowires. Journal of Materials Chemistry C. 2014;**2**(43):9265-9273. DOI: 10.1039/C4TC01632G

[22] Monson C F, Woolley A T. DNA-templated construction of copper nanowires. Nano Letters. 2003; **3**(3):359-363. DOI: 10.1021/nl034016+

[23] Zhang X, Cui Z. Synthesis of Cu nanowires via solventhermal reduction in reverse microemulsion system. Journal of Physics: Conference Series. 2009;**152**(1):012022. DOI: 10.1088/1742 6596/152/1/012022

[24] Shi Y, Li H, Chen L. Obtaining ultra-long copper nanowires via a hydrothermal process. Science and Technology of Advanced Materials. 2005;**6**(7):761-765. DOI: 10.1016/j.stam.2005.06.008

[25] Xu S, Sun X, Ye H. Selective synthesis of copper nanoplates and nanowires via a surfactant-assisted hydrothermal process. Materials Chemistry and Physics. 2010;**120**(1):1-5. DOI: 10.1016/j.matchemphys.2009.10.049

[26] Liu Y, Zhang M, Wang F. Facile microwave-assisted synthesis of uniform single-crystal copper nanowires with excellent electrical conductivity. RSC Advances. 2012;**2**(30):11235-11237. DOI: 10.1039/C2RA21578K

[27] Jiang Z, Tian Y, Ding S. Synthesis and characterization of ultra-long and pencil-like copper nanowires with a penta-twinned structure by hydrothermal method. Materials Letters. 2014;**136**:310-313. DOI: 10.1016/j.matlet.2014.08.033

[28] Ye E, Zhang S, Liu S. Disproportionation for growing copper nanowires and their controlled self-assembly facilitated by ligand exchange. Chemistry – A European Journal. 2011;**17**(11):3074-3077. DOI: 10.1002/chem.201002987

[29] Yang H, He S, Tuan H. Self-seeded growth of five-fold twinned copper nanowires: mechanistic study, characterization, and SERS applications. Langmuir. 2014;**30**(2):602-610. DOI: 10.1021/la4036198

[30] Wang W, Li G, Zhang Z. A facile templateless, surfactantless hydrothermal route to ultralong copper submicron wires. Journal of Crystal Growth. 2007;**299**(1):158-164. DOI: 10.1016/j.jcrysgro.2006.11.221

[31] Zhang X, Zhang D, Ni X. One-step preparation of copper nanorods with rectangular cross sections. Solid State Communications. 2006;**139**(8):412-414. DOI: 10.1016/j.ssc.2006.06.042

[32] Chang Y, Lye M L, Zeng H C. Large-scale synthesis of high-quality ultralong copper nanowires. Langmuir. 2005;**21**(9):3746-3748. DOI: 10.1021/la050220w

[33] Rathmell A R, Bergin S M, Hua Y L. The growth mechanism of copper nanowires and their properties in flexible, transparent conducting films. Advanced Materials. 2010;**22**(32):3558-3563. DOI: 10.1002/adma.201000775

[34] Liu Z, Yang Y, Liang J. Synthesis of copper nanowires via a complex-surfactant-assisted hydrothermal reduction process. The Journal of Physical Chemistry B. 2003;**107**(46):12658-12661. DOI: 10.1021/jp036023s

[35] Ye S, Stewart I E, Chen Z. How copper nanowires grow and how to control their properties. Accounts of Chemical Research. 2016;**49**(3):442-451. DOI: 10.1021/acs.accounts.5b00506

[36] Dou L, Cui F, Yu Y. Solution-processed copper/reduced-graphene-oxide core/shell nanowire transparent conductors. ACS Nano. 2016;**10**(2):2600-2606. DOI: 10.1021/acsnano.5b07651

[37] Mehta R, Chugh S, Chen Z. Enhanced electrical and thermal conduction in graphene-encapsulated copper nanowires. Nano Letters. 2015;**15**(3):2024-2030. DOI: 10.1021/nl504889t

[38] Zhao Y, Zhang Y, Li Y. A flexible chemical vapor deposition method to synthesize copper@carbon core–shell structured nanowires and the study of their structural electrical properties. New Journal of Chemistry. 2012;**36**(5):1161-1169. DOI: 10.1039/c2nj21026f

[39] Zhao Y, Wang J, Zhang Y. The investigation of a hydro-thermal method to fabricate Cu@C coaxial nanowires and their special electronic transport and heat conduction properties. New Journal of Chemistry. 2012;**36**(5):1255-1264. DOI: 10.1039/c2nj40036g

[40] Liu Y, Liu Z, Lu N. Facile synthesis of polypyrrole coated copper nanowires: a new concept to engineered core-shell structures. Chemical Communications. 2012;**48**(20):2621-2623. DOI: 10.1039/c2cc16961d

[41] Liu Z, Elbert D, Chien C. FIB/TEM characterization of the composition and structure of core/shell Cu−Ni nanowires. Nano Letters. 2008;**8**(8):2166-2170. DOI: 10.1021/nl080492u

[42] Alia S M, Yan Y. Palladium coated copper nanowires as a hydrogen oxidation electrocatalyst in base. Journal of the Electrochemical Society. 2015;**162**(8):F849-F853. DOI: 10.1149/2.0211508jes

[43] Alia S M, Jensen K, Contreras C. Platinum coated copper nanowires and platinum nanotubes as oxygen reduction electrocatalysts. ACS Catalysis. 2013;**3**(3):358-362. DOI: 10.1021/cs300664g

[44] Zhang S, Zeng H C. Solution-based epitaxial growth of magnetically responsive Cu@Ni nanowires. Chemistry of Materials. 2010;**22**(4):1282-1284. DOI: 10.1021/cm903105f

[45] Luo X, Gelves G A, Sundararaj U. Silver-coated copper nanowires with improved anti-oxidation property as conductive fillers in low-density polyethylene. The Canadian Journal of Chemical Engineering. 2013;**91**(4):630-637. DOI: 10.1002/cjce.21701

[46] Wei Y, Chen S, Lin Y. Cu–Ag core–shell nanowires for electronic skin with a petal molded microstructure. Journal of Materials Chemistry C. 2015;**3**(37):9594-9602. DOI: 10.1039/c5tc01723h

[47] Wang X, Wang R, Shi L. Synthesis of metal/bimetal nanowires and their applications as flexible transparent electrodes. Small. 2015;**11**(36):4737-4744. DOI: 10.1002/smll.201501314

[48] Stewart I E, Ye S, Chen Z. Synthesis of Cu–Ag, Cu–Au, and Cu–Pt Core–Shell nanowires and their use in transparent conducting films. Chemistry of Materials. 2015;**27**(22):7788-7794. DOI: 10.1021/acs.chemmater.5b03709

[49] Easow J S, Selvaraju T. Unzipped catalytic activity of copper in realizing bimetallic Ag@Cu nanowires as a better amperometric H_2O_2 sensor. Electrochimica Acta. 2013;**112**: 648-654. DOI: 10.1016/j.electacta.2013.09.033

[50] Han M, Liu S, Zhang L, et al. Synthesis of octopus-tentacle-like Cu nanowire-Ag nanocrystals heterostructures and their enhanced electrocatalytic performance for oxygen reduction reaction. ACS Applied Materials & Interfaces. 2012;**4**(12):6654-6660. DOI: 10.1021/am301814y

[51] Zhao J, Zhang D, Zhang X. Preparation and characterization of copper/silver bimetallic nanowires with core-shell structure. Surface and Interface Analysis. 2015;**47**(4):529-534. DOI: 10.1002/sia.5743

[52] Wetzel B, Haupert F, Zhang M. Epoxy nanocomposites with high mechanical and tribological performance. Composites Science and Technology. 2003;**63**(14):2055-2067. DOI: 10.1016/S0266-3538(03)00115-5

IntechOpen